

# $R$ -modes of a neutron star with a magnetic dipole field

Umin Lee<sup>1\*</sup>

<sup>1</sup>*Astronomical Institute, Tohoku University, Sendai, Miyagi 980-8578, Japan*

Typeset 12 December 2018; Received / Accepted

## ABSTRACT

We study  $r$ -modes of a rotating magnetized neutron star, assuming a magnetic dipole field whose axis is aligned with the axis of rotation. We approach the problem by applying a singular perturbation theory to the oscillations of rotating stars. In this treatment, we divide the star into a thin surface magnetic layer and a non-magnetic core. We integrate linearized ideal MHD equations in the surface magnetic layer and non-magnetic oscillation equations in the core, and match the two integrations at the interface to obtain a complete solution. For a polytropic neutron star model of mass  $M = 1.4M_{\odot}$  and radius  $R = 10^6\text{cm}$ , the magnetic dipole field becomes effective on the modal properties of the  $r$ -modes only when the field strength  $B_S$  is much greater than  $10^{14}\text{G}$ . We also find that the damping effects caused by very short magnetic perturbations in the surface layer are not important for the  $r$ -mode instability of rapidly rotating neutron stars if the field strength  $B_S$  is smaller than  $10^{12}\text{G}$ .

**Key words:** instabilities – stars: neutron – stars: oscillations – stars : rotation – stars : magnetic fields

## 1 INTRODUCTION

Several numerical investigations have recently been carried out to study the properties of acoustic modes of magnetized stars (e.g., Dziembowski & Goode 1996, Bigot et al 2000, Cunha & Gough 2000, Saio & Gautschy 2004), particularly for roAp stars (Kurtz 1990). These authors solved the problem of the oscillations of a magnetized star by applying a singular perturbation theory to the stellar oscillation. In their treatment, the stellar interior was divided into the thin surface magnetic layer where the magnetic pressure  $p_m = B^2/8\pi$  is comparable to or greater than the gas pressure  $p$  and the non-magnetic core where the gas pressure is dominant over the magnetic pressure (Biront et al 1982, Roberts & Soward 1983, Cambell & Papaloizou 1986). Linearized ideal MHD equations were integrated in the thin surface magnetic layer, and non-magnetic oscillation equations were integrated in the core, and then the two integrations were matched at the interface between the magnetic and non-magnetic regions to make a complete solution. This treatment is based on the following properties of magnetic perturbations in the interior of stars. If we assume that the gas pressure dominates the magnetic pressure, or equivalently that the Alfvén wave velocity  $v_A = \sqrt{B^2/4\pi\rho}$  is much slower than the sound velocity  $v_S \sim \sqrt{p/\rho}$  in the deep interior, it is reasonable to consider that the magnetic perturbations are largely determined by the induction equation. But, there also exists a component of magnetic perturbations that originates from the Lorentz force term  $\mathbf{j} \times \mathbf{B}$  in the equation of motion. For a typical oscillation frequency of acoustic modes, this component appears as very short magnetic perturbations, the wavelengths of which are much shorter than those of the acoustic modes. In the limit of  $\beta \equiv p/p_m \rightarrow \infty$  in the deep interior, we can expect the short wave component of the magnetic perturbations may be lost from the wave system suffering strong dissipation, which makes it legitimate to divide the stellar interior into a magnetic surface layer and a non-magnetic core and to disregard the short wave component in the core (e.g., Biront et al 1982, Roberts & Soward 1983). If we assume that the oscillation energy imparted by the short magnetic perturbations is lost from the wave system (Biront et al 1982, Roberts & Soward 1983), this *loss* of the magnetic perturbation energies works as a damping mechanism for the acoustic modes. This damping mechanism was implemented in global acoustic mode calculations, for example, by Bigot et al (2000), Cunha & Gough (2000), Saio & Gautschy (2004).

\* E-mail: lee@astr.tohoku.ac.jp

Although the studies mentioned above were all for non-rotating stars, Shibahashi & Takata (1993) and Takata & Shibahashi (1995) have developed a theory of the oscillations of rotating magnetized stars, treating both rotation and the magnetic field as small perturbations to the oscillations of non-rotating and non-magnetic stars. They recognized, however, that the perturbational treatment of the magnetic field in the surface layer might not be justified. Bigot & Dziembowski (2002) have also considered the effects of a magnetic field and rotation on acoustic oscillations. Although they assumed a slow rotation to treat high radial order  $p$ -modes, they employed a non-perturbative approach for the magnetic field, to improve the analyses by Shibahashi & Takata (1993) and Dziembowski & Goode (1996).

$R$ -modes of neutron stars have attracted good attention recently because of the recognition that the  $r$ -modes are driven unstable by the emission of gravitational radiation (Andersson 1998, Friedman & Morsink 1998) due to Chandrasekhar-Friedman-Schutz instability mechanism (Chandrasekhar 1970, Friedman & Schutz 1978 a,b). The  $r$ -modes of rotating neutron stars are expected to be a good candidate for a gravitational wave source (e.g., Andersson & Kokkotas 2004). They are also regarded as a mechanism that decelerates the spin of young neutron stars, since the gravitational radiation carries away angular momentum of the star (e.g., Owen et al 1998). However, before we draw a decisive conclusion concerning the role played by the  $r$ -modes in neutron star physics, we need to examine how strongly the modal properties are affected by various physical factors such as viscosity, solid crust, superfluidity, general relativity, nonlinear amplitude saturation, and so on. A magnetic field of the star is one of such influential factors.

$R$ -mode oscillations of rotating magnetized neutron stars have been discussed by Rezzolla, Lamb, & Shapiro (2000), Ho & Lai (2000), and Morsink & Reznia (2002). For example, Ho & Lai (2000) estimated the shifts of the  $r$ -mode frequency caused by the strong magnetic field using a local linear analysis, suggesting that the oscillation manifests itself as Rossby waves in the bulk interior, but assumes the Alfvén wave character near the stellar surface. Morsink & Reznia (2002) developed, based on the formalism introduced by Schenk et al (2002), a formalism to compute the magnetically modified global  $r$ -modes, without assuming a weak magnetic field of the star. In this paper, we approach the problem of the oscillations of a rotating magnetized star by applying a singular perturbation theory to the oscillations of a rotating non-magnetic star (e.g., Lee & Saio 1986). In §2, we derive the oscillation equations of a rotating magnetized star, assuming the axis of the dipole field is aligned with the axis of rotation. §3 is for numerical results, and §4 is for discussions and conclusions.

## 2 METHOD OF SOLUTION

### 2.1 Oscillation equations of a rotating star with a magnetic dipole field

In this paper, we assume adiabatic oscillations of a uniformly rotating star and employ the Cowling approximation, neglecting the Euler perturbation of the gravitational potential. We also assume that the axis of the magnetic dipole field is aligned with that of rotation. If we employ spherical polar coordinates  $(r, \theta, \phi)$  whose origin is at the center of the star, a magnetic dipole field may be given by

$$\mathbf{B} = \mu \nabla (\cos \theta / r^2), \quad (1)$$

where  $\mu$  is the magnetic dipole moment, and we have assumed that the axis of the field corresponds to the coordinate axis defined by  $\theta = 0$ . When the axes of rotation and the magnetic field are aligned, it is possible to assume that the equilibrium state is axisymmetric with respect to the axis  $\theta = 0$ , and that the time and azimuthal angular dependence of the perturbations is given by  $e^{i\sigma t + im\phi}$ , where  $\sigma$  is the oscillation frequency in an inertial frame and  $m$  is an integer representing the azimuthal wave number. Note that the magnetic dipole field is a force free field (i.e.,  $(\nabla \times \mathbf{B}) \times \mathbf{B} = 0$ ) and does not affect the equilibrium structure of the star. Since we are interested in low frequency oscillations in this paper, we neglect the effects of rotational deformation. Linearized ideal MHD equations with infinite conductivity may be given by (e.g., Unno et al 1989)

$$-\omega^2 \boldsymbol{\xi} = -\frac{1}{\rho} \nabla p' + \frac{\rho'}{\rho^2} \nabla p - 2i\omega \boldsymbol{\Omega} \times \boldsymbol{\xi} + \frac{1}{4\pi\rho} (\nabla \times \mathbf{B}') \times \mathbf{B}, \quad (2)$$

$$\rho' + \nabla \cdot (\rho \boldsymbol{\xi}) = 0, \quad (3)$$

$$\mathbf{B}' = \nabla \times (\boldsymbol{\xi} \times \mathbf{B}), \quad (4)$$

and for adiabatic pulsations

$$\frac{\rho'}{\rho} = \frac{1}{\Gamma_1} \frac{p'}{p} - \xi_r A, \quad (5)$$

where  $\rho$  is the mass density,  $p$  is the pressure,  $\boldsymbol{\Omega}$  is the angular velocity of rotation,  $\mathbf{B}$  is the magnetic field, and the physical quantities with a prime ( $'$ ) denote their Euler perturbations,  $\boldsymbol{\xi}$  is the displacement vector, and  $\omega = \sigma + m\Omega$  denotes the oscillation frequency observed in the corotating frame of the star. Here,  $A$  is the Schwartzschild discriminant defined by

$$A = \frac{d \ln \rho}{dr} - \frac{1}{\Gamma_1} \frac{d \ln p}{dr}, \quad (6)$$

where

$$\Gamma_1 = \left( \frac{\partial \ln p}{\partial \ln \rho} \right)_{ad}. \quad (7)$$

To represent the angular dependence of the perturbations of a rotating magnetized star, we expand the perturbed quantities in terms of spherical harmonic functions with different degrees  $l$  for a given  $m$ . The displacement vector  $\boldsymbol{\xi}$  is then given by

$$\xi_r = \sum_{j=1}^{\infty} S_{l_j}(r) Y_{l_j}^m(\theta, \phi) e^{i\sigma t}, \quad (8)$$

$$\xi_\theta = \sum_{j=1}^{\infty} \left[ H_{l_j}(r) \frac{\partial}{\partial \theta} Y_{l_j}^m(\theta, \phi) + T_{l'_j}(r) \frac{1}{\sin \theta} \frac{\partial}{\partial \phi} Y_{l'_j}^m(\theta, \phi) \right] e^{i\sigma t}, \quad (9)$$

$$\xi_\phi = \sum_{j=1}^{\infty} \left[ H_{l_j}(r) \frac{1}{\sin \theta} \frac{\partial}{\partial \phi} Y_{l_j}^m(\theta, \phi) - T_{l'_j}(r) \frac{\partial}{\partial \theta} Y_{l'_j}^m(\theta, \phi) \right] e^{i\sigma t}, \quad (10)$$

and the perturbed magnetic field  $\mathbf{B}'$  is given by

$$B'_r = B_0(r) \sum_{j=1}^{\infty} b_{l'_j}^S(r) Y_{l'_j}^m(\theta, \phi) e^{i\sigma t}, \quad (11)$$

$$B'_\theta = B_0(r) \sum_{j=1}^{\infty} \left[ b_{l'_j}^H(r) \frac{\partial}{\partial \theta} Y_{l'_j}^m(\theta, \phi) + b_{l'_j}^T(r) \frac{1}{\sin \theta} \frac{\partial}{\partial \phi} Y_{l'_j}^m(\theta, \phi) \right] e^{i\sigma t}, \quad (12)$$

$$B'_\phi = B_0(r) \sum_{j=1}^{\infty} \left[ b_{l'_j}^H(r) \frac{1}{\sin \theta} \frac{\partial}{\partial \phi} Y_{l'_j}^m(\theta, \phi) - b_{l'_j}^T(r) \frac{\partial}{\partial \theta} Y_{l'_j}^m(\theta, \phi) \right] e^{i\sigma t}, \quad (13)$$

and a perturbed scalar quantity such as  $p'$  is given by

$$p' = \sum_{j=1}^{\infty} p'_{l_j}(r) Y_{l_j}^m(\theta, \phi) e^{i\sigma t}. \quad (14)$$

where  $B_0(r) = \mu/r^3$ , and  $l_j = |m| + 2(j-1)$  and  $l'_j = l_j + 1$  for even modes, and  $l_j = |m| + 2j - 1$  and  $l'_j = l_j - 1$  for odd modes, respectively, and  $j = 1, 2, 3, \dots$ .

Substituting the expansions into the linearized basic equations (2) to (5), we obtain a set of coupled ordinary linear differential equations of infinite dimension for the expansion coefficients. If we use for the expansion coefficients vector notation given by

$$(\mathbf{y}_1)_j = S_{l_j}/r, \quad (\mathbf{y}_2)_j = p'_{l_j}/\rho g r, \quad (\mathbf{b}^S)_j = b_{l'_j}^S, \quad (\mathbf{b}^H)_j = b_{l'_j}^H, \quad (\mathbf{b}^T)_j = b_{l'_j}^T, \quad (\mathbf{h})_j = H_{l_j}/r, \quad (\mathbf{t})_j = T_{l'_j}/r, \quad (15)$$

the oscillation equations of a rotating star with an aligned magnetic dipole field are given in the Cowling approximation as

$$r \frac{d\mathbf{y}_1}{dr} = (V_G - 3) \mathbf{y}_1 - V_G \mathbf{y}_2 + \Lambda_0 \mathbf{h}, \quad (16)$$

$$\begin{aligned} r \frac{d\mathbf{y}_2}{dr} &= (c_1 \bar{\omega}^2 + rA) \mathbf{y}_1 + (1 - rA - U) \mathbf{y}_2 - 2mc_1 \bar{\omega} \bar{\Omega} \mathbf{h} - 2c_1 \bar{\omega} \bar{\Omega} C_0 i \mathbf{t} \\ &+ \frac{c_1 \bar{\omega}^2}{2} \left( C_0 r \frac{d}{dr} \frac{\mathbf{b}^H}{\alpha} + mr \frac{d}{dr} \frac{i \mathbf{b}^T}{\alpha} - f C_0 \frac{\mathbf{b}^H}{\alpha} - mf \frac{i \mathbf{b}^T}{\alpha} - C_0 \frac{\mathbf{b}^S}{\alpha} \right), \end{aligned} \quad (17)$$

$$\begin{aligned} r \frac{d}{dr} \begin{pmatrix} \mathbf{b}^H/\alpha \\ i \mathbf{b}^T/\alpha \end{pmatrix} &= \begin{pmatrix} m\nu G_1^{-1}(K + M_0) - \Lambda_1 K/\alpha & G_1^{-1} M_0 \Lambda_0 / c_1 \bar{\omega}^2 \\ -\nu G_0^{-1}(m^2 \Lambda_0^{-1} + M_1 \Lambda_1 K) & -m G_0^{-1} / c_1 \bar{\omega}^2 \end{pmatrix} \begin{pmatrix} \mathbf{y}_1 \\ \mathbf{y}_2 \end{pmatrix} \\ &+ \begin{pmatrix} f \mathbf{1} & -m G_1^{-1}(C_1 + M_0 \Lambda_0)/2 \\ 0 & f \mathbf{1} + G_0^{-1}(m^2 \mathbf{1} + M_1 \Lambda_1 C_1)/2 \end{pmatrix} \begin{pmatrix} \mathbf{b}^H/\alpha \\ i \mathbf{b}^T/\alpha \end{pmatrix} + \begin{pmatrix} -G_1^{-1} M_0 \Lambda_0 - 2\Lambda_1 M_0/\alpha & m G_1^{-1} - (\nu + 2m/\alpha) \mathbf{1} \\ m G_0^{-1} - \nu \mathbf{1} & -G_0^{-1} M_1 \Lambda_1 \end{pmatrix} \begin{pmatrix} \mathbf{h} \\ i \mathbf{t} \end{pmatrix}, \end{aligned} \quad (18)$$

$$\begin{aligned} r \frac{d}{dr} \begin{pmatrix} \mathbf{h} \\ i \mathbf{t} \end{pmatrix} &= \frac{1}{2} \begin{pmatrix} (V_G - 4) G_0^{-1}(m^2 \Lambda_0^{-1} + M_1 \Lambda_1 K) & -V_G G_0^{-1}(m^2 \Lambda_0^{-1} + M_1 \Lambda_1 K) \\ -m(V_G - 4) G_1^{-1}(K + M_0) & m V_G G_1^{-1}(K + M_0) \end{pmatrix} \begin{pmatrix} \mathbf{y}_1 \\ \mathbf{y}_2 \end{pmatrix} \\ &+ \frac{\alpha}{2} \begin{pmatrix} G_0^{-1} M_1 \Lambda_1 & -m G_0^{-1} \\ -m G_1^{-1} & G_1^{-1} M_0 \Lambda_0 \end{pmatrix} \begin{pmatrix} \mathbf{b}^H/\alpha \\ i \mathbf{b}^T/\alpha \end{pmatrix} + \begin{pmatrix} \mathbf{1} + G_0^{-1} M_1 \Lambda_1 C_1/2 & -m G_0^{-1} C_0/2 \\ -m G_1^{-1} C_1/2 & \mathbf{1} + G_1^{-1} M_0 \Lambda_0 C_0/2 \end{pmatrix} \begin{pmatrix} \mathbf{h} \\ i \mathbf{t} \end{pmatrix}, \end{aligned} \quad (19)$$

$$\mathbf{b}^S = -\Lambda_1 K \mathbf{y}_1 - 2\Lambda_1 M_0 \mathbf{h} - 2m i t, \quad (20)$$

where  $\nu = 2\Omega/\omega$ , and  $\bar{\omega} = \omega/\sqrt{GM/R^3}$  and  $\bar{\Omega} = \Omega/\sqrt{GM/R^3}$  with  $M$  and  $R$  being the mass and the radius of the star, and

$$U = \frac{d \ln M_r}{d \ln r}, \quad V = -\frac{d \ln p}{d \ln r}, \quad V_G = \frac{V}{\Gamma_1}, \quad c_1 = \frac{(r/R)^3}{M_r/M}, \quad (21)$$

and

$$\alpha = \frac{c_1 \bar{\omega}^2 \beta V}{4}, \quad \beta = \frac{p}{B_0^2/8\pi}, \quad f = 2 - \frac{d \ln \alpha}{d \ln r}. \quad (22)$$

Here, equation (16) comes from the continuity equation (3), equations (17) and (18) from the radial and the horizontal components of the equation of motion (2), and equations (19) and (20) from the induction equation (4). The matrices  $G_0$  and  $G_1$  are defined as

$$G_0 = m^2 \Lambda_0^{-1} - M_1 \Lambda_1 M_0, \quad G_1 = m^2 \Lambda_1^{-1} - M_0 \Lambda_0 M_1, \quad (23)$$

and the non-zero elements of the matrices  $M_0$ ,  $M_1$ ,  $C_0$ , and  $C_1$  are given by

$$(M_0)_{j,j} = \frac{l_j}{l_j+1} J_{l_j+1}^m, \quad (M_0)_{j,j+1} = \frac{l_j+3}{l_j+2} J_{l_j+2}^m, \quad (M_1)_{j,j} = \frac{l_j+2}{l_j+1} J_{l_j+1}^m, \quad (M_1)_{j+1,j} = \frac{l_j+1}{l_j+2} J_{l_j+2}^m, \quad (24)$$

$$(C_0)_{j,j} = -(l_j+2) J_{l_j+1}^m, \quad (C_0)_{j+1,j} = (l_j+1) J_{l_j+2}^m, \quad (C_1)_{j,j} = l_j J_{l_j+1}^m, \quad (C_1)_{j+1,j} = -(l_j+3) J_{l_j+2}^m, \quad (25)$$

for even modes, and

$$(M_0)_{j,j} = \frac{l_j+1}{l_j} J_{l_j}^m, \quad (M_0)_{j+1,j} = \frac{l_j}{l_j+1} J_{l_j+1}^m, \quad (M_1)_{j,j} = \frac{l_j-1}{l_j} J_{l_j}^m, \quad (M_1)_{j+1,j} = \frac{l_j+2}{l_j+1} J_{l_j+1}^m, \quad (26)$$

$$(C_0)_{j,j} = (l_j-1) J_{l_j}^m, \quad (C_0)_{j+1,j} = -(l_j+2) J_{l_j+1}^m, \quad (C_1)_{j,j} = -(l_j+1) J_{l_j}^m, \quad (C_1)_{j+1,j} = l_j J_{l_j+1}^m, \quad (27)$$

for odd modes, and  $\mathbf{1}$  denotes the unit matrix. The definition of the matrices  $K$ ,  $L_0$ ,  $L_1$ ,  $\Lambda_0$ ,  $\Lambda_1$  is the same as that given in Lee & Saio (1990).

The oscillation equations derived above are integrated in the thin surface magnetic layer, and non-magnetic oscillation equations (e.g., Lee & Saio 1986) are integrated in the non-magnetic core. The two integrations are matched at the interface between the magnetic and non-magnetic regions to obtain a complete solution.

For numerical computation, we solve a finite set of the linear ordinary differential equations, which is derived by truncating the infinite expansions of perturbed quantities so that the first  $k_{max}$  expansion coefficients with  $l_j$  and  $l'_j$  from  $j = 1$  to  $j = k_{max}$  are retained for each quantity. In most cases, we employ  $k_{max} = 6$  in this paper. Using a relaxation method (e.g., Unno et al 1989), we solve as an eigenvalue problem for  $\bar{\omega}$  the finite set of linear differential equations with appropriate boundary conditions at the center and the surface of the star and jump conditions at the interface (see the next subsection).

## 2.2 Boundary conditions and jump conditions

The surface boundary conditions we use are

$$\delta p/p = 0, \quad i\mathbf{b}^T = 0, \quad \mathbf{b}^S + L^+ \mathbf{b}^H = 0, \quad (28)$$

where  $\delta p$  is the Lagrangian perturbation of the pressure, and  $(L^+)_{ij} = \delta_{ij}(l'_j + 1)$ . The latter two conditions come from the assumption that the perturbed magnetic field must be continuous to the outside field that is given by a scalar potential (i.e.,  $\nabla \times \mathbf{B}' = 0$ ; Cambell & Papaloizou 1986, Cunha & Gough 2000, Saio & Gautschi 2004). The inner boundary condition at the stellar center is the regularity condition of the functions  $\mathbf{y}_1$  and  $\mathbf{y}_2$  (e.g., Lee & Saio 1986).

The jump conditions we apply at the interface are the continuity of the functions  $\mathbf{y}_1$  and  $\mathbf{y}_2$ , and the condition that the oscillation energy imparted by the perturbed magnetic field is lost from the wave system. To consider the latter condition, it is instructive to differentiate equation (18) with respect to  $\ln r$  to obtain

$$r \frac{d}{dr} r \frac{d}{dr} \begin{pmatrix} \mathbf{b}^H/\alpha \\ i\mathbf{b}^T/\alpha \end{pmatrix} = -\frac{\alpha}{2} \begin{pmatrix} -G_1^{-1} M_0 \Lambda_0 & mG_1^{-1} - \nu \mathbf{1} \\ mG_0^{-1} - \nu \mathbf{1} & -G_0^{-1} M_1 \Lambda_1 \end{pmatrix} \begin{pmatrix} -G_0^{-1} M_1 \Lambda_1 & mG_0^{-1} \\ mG_1^{-1} & -G_1^{-1} M_0 \Lambda_0 \end{pmatrix} \begin{pmatrix} \mathbf{b}^H/\alpha \\ i\mathbf{b}^T/\alpha \end{pmatrix} + \dots \quad (29)$$

where we have used equations (16)  $\sim$  (20) to eliminate  $\mathbf{h}$  and  $i\mathbf{t}$ . Since the quantity  $|\alpha|$  can be very large in the interior, if we assume a WKB type solution in the region near the interface such that  $(\mathbf{b}^H/\alpha, i\mathbf{b}^T/\alpha) \propto \exp(ik_r \ln r + im\phi + i\omega t)$ , we obtain the wavenumber  $k_r \propto \sqrt{\alpha}$ , which suggests the existence of very short magnetic perturbations. These short magnetic perturbations are attributable to the Alfvén waves. In the deep interior where the gas pressure dominates the magnetic pressure so that  $\beta \gg 1$ , it may be legitimate to write

$$\begin{pmatrix} \mathbf{b}^H/\alpha \\ i\mathbf{b}^T/\alpha \end{pmatrix} = \begin{pmatrix} \mathbf{b}^H/\alpha \\ i\mathbf{b}^T/\alpha \end{pmatrix}_0 + \begin{pmatrix} \mathbf{b}^H/\alpha \\ i\mathbf{b}^T/\alpha \end{pmatrix}_m, \quad \begin{pmatrix} \mathbf{h} \\ i\mathbf{t} \end{pmatrix} = \begin{pmatrix} \mathbf{h} \\ i\mathbf{t} \end{pmatrix}_0 + \begin{pmatrix} \mathbf{h} \\ i\mathbf{t} \end{pmatrix}_m, \quad \begin{pmatrix} \mathbf{y}_1 \\ \mathbf{y}_2 \end{pmatrix} = \begin{pmatrix} \mathbf{y}_1 \\ \mathbf{y}_2 \end{pmatrix}_0, \quad (30)$$

where the functions with a subscript 0 denote non-Alfvénic perturbations and those with a subscript  $m$  denote the Alfvénic perturbations, and the former are assumed to have wavelengths much longer than the latter. For the non-Alfvénic perturbations in the deep interior, we assume

$$\begin{pmatrix} -G_1^{-1}M_0\Lambda_0 & mG_1^{-1} - \nu\mathbf{1} \\ mG_0^{-1} - \nu\mathbf{1} & -G_0^{-1}M_1\Lambda_1 \end{pmatrix} \begin{pmatrix} \mathbf{h} \\ i\mathbf{t} \end{pmatrix}_0 = - \begin{pmatrix} m\nu G_1^{-1}(K + M_0) & G_1^{-1}M_0\Lambda_0/c_1\bar{\omega}^2 \\ -\nu G_0^{-1}(m^2\Lambda_0^{-1} + M_1\Lambda_1 K) & -mG_0^{-1}/c_1\bar{\omega}^2 \end{pmatrix} \begin{pmatrix} \mathbf{y}_1 \\ \mathbf{y}_2 \end{pmatrix}_0, \quad (31)$$

which is equivalent to equations (A4) and (A5) in Lee & Saio (1990), and

$$\begin{aligned} \frac{1}{2} \begin{pmatrix} G_0^{-1}M_1\Lambda_1 & -mG_0^{-1} \\ -mG_1^{-1} & G_1^{-1}M_0\Lambda_0 \end{pmatrix} \begin{pmatrix} \mathbf{b}^H \\ i\mathbf{b}^T \end{pmatrix}_0 &= r \frac{d}{dr} \begin{pmatrix} \mathbf{h} \\ i\mathbf{t} \end{pmatrix}_0 - \begin{pmatrix} \mathbf{1} + G_0^{-1}M_1\Lambda_1 C_1/2 & -mG_0^{-1}C_0/2 \\ -mG_1^{-1}C_1/2 & \mathbf{1} + G_1^{-1}M_0\Lambda_0 C_0/2 \end{pmatrix} \begin{pmatrix} \mathbf{h} \\ i\mathbf{t} \end{pmatrix}_0 \\ -\frac{1}{2} \begin{pmatrix} (V_G - 4)G_0^{-1}(m^2\Lambda_0^{-1} + M_1\Lambda_1 K) & -V_G G_0^{-1}(m^2\Lambda_0^{-1} + M_1\Lambda_1 K) \\ -m(V_G - 4)G_1^{-1}(K + M_0) & mV_G G_1^{-1}(K + M_0) \end{pmatrix} \begin{pmatrix} \mathbf{y}_1 \\ \mathbf{y}_2 \end{pmatrix}_0, \end{aligned} \quad (32)$$

which comes from equation (4) assuming  $\beta \gg 1$  (see §4). Using equations (30) to (32) in equations (18) and (19), we obtain for the Alfvénic perturbations

$$\begin{aligned} r \frac{d}{dr} \begin{pmatrix} \mathbf{b}^H/\alpha \\ i\mathbf{b}^T/\alpha \end{pmatrix}_m &= \begin{pmatrix} f\mathbf{1} & -mG_1^{-1}(C_1 + M_0\Lambda_0)/2 \\ 0 & f\mathbf{1} + G_0^{-1}(m^2\mathbf{1} + M_1\Lambda_1 C_1)/2 \end{pmatrix} \begin{pmatrix} \mathbf{b}^H/\alpha \\ i\mathbf{b}^T/\alpha \end{pmatrix}_m + \begin{pmatrix} -G_1^{-1}M_0\Lambda_0 & mG_1^{-1} - \nu\mathbf{1} \\ mG_0^{-1} - \nu\mathbf{1} & -G_0^{-1}M_1\Lambda_1 \end{pmatrix} \begin{pmatrix} \mathbf{h} \\ i\mathbf{t} \end{pmatrix}_m \\ + \begin{pmatrix} f\mathbf{1} & -mG_1^{-1}(C_1 + M_0\Lambda_0)/2 \\ 0 & f\mathbf{1} + G_0^{-1}(m^2\mathbf{1} + M_1\Lambda_1 C_1)/2 \end{pmatrix} \begin{pmatrix} \mathbf{b}^H/\alpha \\ i\mathbf{b}^T/\alpha \end{pmatrix}_0 - r \frac{d}{dr} \begin{pmatrix} \mathbf{b}^H/\alpha \\ i\mathbf{b}^T/\alpha \end{pmatrix}_0 + \begin{pmatrix} \mathbf{b}^S/\alpha \\ 0 \end{pmatrix}_0, \end{aligned} \quad (33)$$

$$r \frac{d}{dr} \begin{pmatrix} \mathbf{h} \\ i\mathbf{t} \end{pmatrix}_m = \frac{\alpha}{2} \begin{pmatrix} G_0^{-1}M_1\Lambda_1 & -mG_0^{-1} \\ -mG_1^{-1} & G_1^{-1}M_0\Lambda_0 \end{pmatrix} \begin{pmatrix} \mathbf{b}^H/\alpha \\ i\mathbf{b}^T/\alpha \end{pmatrix}_m + \begin{pmatrix} \mathbf{1} + G_0^{-1}M_1\Lambda_1 C_1/2 & -mG_0^{-1}C_0/2 \\ -mG_1^{-1}C_1/2 & \mathbf{1} + G_1^{-1}M_0\Lambda_0 C_0/2 \end{pmatrix} \begin{pmatrix} \mathbf{h} \\ i\mathbf{t} \end{pmatrix}_m. \quad (34)$$

Defining

$$\mathbf{Y}_m = \begin{pmatrix} \mathbf{b}^H/\alpha \\ \mathbf{b}^T/\alpha \\ \mathbf{h} \\ i\mathbf{t} \end{pmatrix}_m, \quad \mathbf{y}_0 = \begin{pmatrix} \mathbf{y}_1 \\ \mathbf{y}_2 \end{pmatrix}_0, \quad (35)$$

we may formally rewrite equations (33) and (34) as

$$r \frac{d}{dr} \mathbf{Y}_m = A \mathbf{Y}_m + B \mathbf{y}_0, \quad (36)$$

where equations (31) and (32) have been used to eliminate  $(\mathbf{b}_0^H, i\mathbf{b}_0^T)$  and  $(\mathbf{h}_0, i\mathbf{t}_0)$ , and matrices  $A$  and  $B$  are determined by equations (33) and (34). Here, we regard equation (36) as a linear differential equation of  $\mathbf{Y}_m$  with an inhomogeneous term  $B\mathbf{y}_0$ . The homogeneous part of the linear differential equation is solved by assuming  $\mathbf{Y}_m \propto e^{ik_r \ln r}$ , where the wavenumber  $k_r$  is obtained as eigenvalues to the equation  $ik_r \mathbf{Y}_m = A \mathbf{Y}_m$ .

To make the discussion more concrete, let us now consider a finite set of the linear differential equations, which is obtained by truncating the infinite expansions of perturbed quantities, keeping the first  $k_{max}$  expansion coefficients for each perturbed quantity. In this case, the dimension of the vector  $\mathbf{Y}_m$  is  $4k_{max}$ , and the number of eigenvalues  $k_r$  to  $ik_r \mathbf{Y}_m = A \mathbf{Y}_m$  is also  $4k_{max}$ . To construct jump conditions at the interface, we pick up  $N = 2k_{max}$  eigenvalues  $k_r^j$  and the eigenfunctions  $\mathbf{Y}_m^j$  that satisfy the condition

$$\text{Re}(k_r^j) < 0 \quad \text{and} \quad |\text{Re}(k_r^j)| > |\text{Im}(k_r^j)|, \quad (37)$$

or

$$\text{Im}(k_r^j) < 0 \quad \text{and} \quad |\text{Im}(k_r^j)| > |\text{Re}(k_r^j)|, \quad (38)$$

and write a general solution to equation (36) as

$$\mathbf{Y}_m = \sum_{j=1}^N c_j \mathbf{Y}_m^j e^{ik_r^j \ln r} - A^{-1} B \mathbf{y}_0 = (\mathbf{Y}_m^1, \dots, \mathbf{Y}_m^N) \begin{pmatrix} c^1 e^{k_r^1 \ln r} \\ \vdots \\ c^N e^{k_r^N \ln r} \end{pmatrix} - A^{-1} B \mathbf{y}_0 \quad (39)$$

where  $-A^{-1}B\mathbf{y}_0$  is a special solution to equation (36), and  $c^j$ 's are arbitrary constants. The condition (37) means that the Alfvénic perturbations are chosen to be running waves into the core (e.g., Saio & Gautschi 2004). It is important to note that, different from the case of acoustic modes, the number of the eigenvalues  $k_r^j$  that satisfy  $\text{Re}(k_r) < 0$  and  $|\text{Re}(k_r)| > |\text{Im}(k_r)|$  is usually less than  $N = 2k_{max}$  for rotational modes. This is the reason why we add the eigenvalues  $k_r^j$  that satisfy  $\text{Im}(k_r) < 0$  and  $|\text{Im}(k_r)| > |\text{Re}(k_r)|$  to make the total number of the conditions equal to  $N$ . Splitting the solution (39) into the upper and the lower parts so that  $(\mathbf{Y}_m^1, \dots, \mathbf{Y}_m^N)_U$  and  $(\mathbf{Y}_m^1, \dots, \mathbf{Y}_m^N)_L$  become square matrices of dimension  $2k_{max} \times 2k_{max}$ , we have

**Table 1.** Complex eigenvalue  $\kappa = \bar{\omega}/\bar{\Omega}$  and the frequency deviation  $(\kappa_R - \kappa_0)/\kappa_0$  of the  $l' = |m|$   $r$ -modes at  $\bar{\Omega} = 0.1$ .

$B_S(\text{G})$	$m = 1$				$m = 2$			
	$\kappa_R$	$\kappa_I$	$(\kappa_R - \kappa_0)/\kappa_0$	$x_i$	$\kappa_R$	$\kappa_I$	$(\kappa_R - \kappa_0)/\kappa_0$	$x_i$
$10^{12}$	0.99642	$2.7 \times 10^{-13}$	$1.5 \times 10^{-11}$	0.998	0.66517	$1.1 \times 10^{-10}$	$2.4 \times 10^{-9}$	0.997
$10^{14}$	0.99642	$5.0 \times 10^{-9}$	$-1.8 \times 10^{-8}$	0.98	0.66518	$9.5 \times 10^{-7}$	$1.8 \times 10^{-5}$	0.98

$$(\mathbf{Y}_m + A^{-1}B\mathbf{y}_0)_U = (\mathbf{Y}_m^1, \dots, \mathbf{Y}_m^N)_U \begin{pmatrix} c^1 e^{k_r^1 \ln r} \\ \vdots \\ c^N e^{k_r^N \ln r} \end{pmatrix}, \quad (40)$$

and

$$(\mathbf{Y}_m + A^{-1}B\mathbf{y}_0)_L = (\mathbf{Y}_m^1, \dots, \mathbf{Y}_m^N)_L \begin{pmatrix} c^1 e^{k_r^1 \ln r} \\ \vdots \\ c^N e^{k_r^N \ln r} \end{pmatrix}. \quad (41)$$

Eliminating the arbitrary constants  $c^j$  between equations (40) and (41), we finally obtain (e.g., Saio & Gautschi 2004)

$$(\mathbf{Y}_m^1, \dots, \mathbf{Y}_m^N)_U^{-1} (\mathbf{Y}_m + A^{-1}B\mathbf{y}_0)_U = (\mathbf{Y}_m^1, \dots, \mathbf{Y}_m^N)_L^{-1} (\mathbf{Y}_m + A^{-1}B\mathbf{y}_0)_L, \quad (42)$$

where  $\mathbf{Y}_m$  is to be replaced by  $\mathbf{Y} - \mathbf{Y}_0$  with  $\mathbf{Y}_0 = (b_0^H, ib_0^T, \mathbf{h}_0, it_0)$ . The number of jump conditions supplied by equation (42) is  $N$ , and since the continuity of the functions  $\mathbf{y}_1$  and  $\mathbf{y}_2$  at the interface gives  $N$  jump conditions, we have in total  $2N$  conditions at the interface.

### 3 NUMERICAL RESULTS

$R$ -modes of non-magnetic polytropes were investigated, for example, by Yoshida & Lee (2000a,b). The Coriolis force is the restoring force, and the oscillation frequency  $\omega$  is proportional to the rotation frequency  $\Omega$ . The  $r$ -modes are retrograde modes, in the corotating frame of the star, having the asymptotic frequency  $\omega = 2m\Omega/[l'(l' + 1)]$  for  $\Omega \rightarrow 0$  for given  $m$  and  $l'$ , and the eigenfunctions are dominated by the toroidal component  $iT_{l'}$  of the displacement vector  $\boldsymbol{\xi}$ . For isentropic stars, the odd  $r$ -mode with  $l' = |m|$  is the only  $r$ -mode for a given  $m$ , and the eigenfunctions are dominated by the nodeless toroidal component  $iT_{|m|}$ .

For neutron star models, we employ an  $N = 1$  polytrope of mass  $M = 1.4M_\odot$  and radius  $R = 10^6 \text{ cm}$ , for which we assume  $\Gamma_1 = 1 + 1/N$  so that the Schwartzschild discriminant  $A$  vanishes in the interior. As discussed in the previous section, the radial wavenumber of Alfvénic perturbations near the interface may be approximately given by

$$|k_r| \sim \sqrt{\alpha/2} = t_A \omega / 2 \propto |\bar{\omega}| / B_S, \quad (43)$$

where  $B_S = B_0(R)$ , and  $t_A = r/v_A$  with  $v_A = \sqrt{B^2/4\pi\rho}$  being the Alfvén velocity denotes the traveling time for the Alfvén waves. This equation indicates that Alfvénic perturbations have very short wavelengths  $\sim 1/k_r$  if the traveling time of the Alfvén waves is much longer than the typical oscillation period of the modes. Figure 1 gives the quantity  $\sqrt{\alpha}$  as a function of  $x = r/R$  for  $B_S = 10^{12} \text{ G}$  (solid line),  $B_S = 10^{14} \text{ G}$  (dashed line), and  $B_S = 10^{16} \text{ G}$  (dash-dotted line), assuming  $\bar{\omega} = 1$ . This figure shows that, as the depth  $z \equiv R - r$  from the surface increases, the radial wavenumber  $k_r$  of Alfvénic perturbations increases quite rapidly and becomes as large as  $10^4 \sim 10^5$  beneath the surface, indicating that the travelling time of the Alfvén waves in a typical neutron star model with  $B_S \lesssim 10^{14} \text{ G}$  is much longer than the oscillation period of rotational modes unless  $\bar{\omega} \sim 0$ . Since the Alfvénic perturbations associated with the  $r$ -modes have very short wavelengths for  $B_S \lesssim 10^{14} \text{ G}$ , we have to allocate a large number of mesh points to describe them correctly even in the thin surface region.

In Table 1, we tabulate the complex eigenvalue  $\kappa \equiv \omega/\Omega = \kappa_R + i\kappa_I$  and the frequency deviation  $(\kappa_R - \kappa_0)/\kappa_0$  for the  $r$ -modes of  $m = 1$  and  $m = 2$  at  $\bar{\Omega} = 0.1$  for  $B_S = 10^{12} \text{ G}$  and  $B_S = 10^{14} \text{ G}$ , where  $\kappa_0$  denotes the eigenvalue of the non-magnetic  $r$  modes, and  $x_i \equiv r_i/R$  and  $r_i$  is the radial distance of the interface from the stellar center. Here, we use  $k_{max} = 6$  for Table 1. Note that the location  $x_i$  of the interface for the case of  $B_S = 10^{14} \text{ G}$  is deeper than that for  $B_S = 10^{12} \text{ G}$ . We find that the eigenvalue  $\kappa_R$  of the  $r$ -modes is hardly affected by the magnetic field of strength  $B_S \lesssim 10^{14} \text{ G}$ . This is because the Alfvénic perturbations become decoupled from the  $r$ -modes immediately beneath the surface, giving only a skin effect on the modes. If we consider a magnetic field as strong as  $B_S \gtrsim 10^{16}$ , the wavelengths of the Alfvénic perturbations will be comparable to the radius of the star for rotational modes of  $\bar{\omega} \sim \bar{\Omega} \lesssim 1$ , and no decoupling of the Alfvénic perturbations from the rotational modes will be expected in a thin surface layer. In this case, the method of calculation applied in this paper may not be justified, but the linearized MHD equations need to be integrated in the entire interior of the star to determine the eigensolutions.

Table 1 also shows that the  $r$ -modes are stable having positive  $\kappa_I$ , which is, however, quite small for the strength of the field considered in this paper. Although the magnetic effects on the eigenfrequency are weak, it is important to note that the effects are larger for the larger  $B_S$ , and that the  $r$ -mode of  $m = 1$  is less influenced by the dipole field than that of  $m = 2$ , as indicated by Table 1.

For the case of  $B_S = 10^{12}$  G, the real parts of the eigenfunctions of the  $r$ -mode of  $m = 1$  are plotted versus  $r/R$  in Figures 2 to 4, and those of the  $r$ -mode of  $m = 2$  in Figures 5 to 7, where we assume  $\bar{\Omega} = 0.1$  and  $k_{max} = 6$ , and we employ the amplitude normalization given by  $S_{l_1} = 1$  at the surface. The presence of the magnetic dipole field of strength  $B_S = 10^{12}$  G has practically no influence on the modal properties of the modes. The magnetic  $r$ -mode has the dominant toroidal component  $iT_{l'=|m|}$  of the displacement vector over the horizontal  $H_{l=|m|+1}$  and radial  $S_{l=|m|+1}$  components, and the amplitudes of the radial and horizontal components are almost the same order of magnitude at the surface. The Alfvénic perturbations  $(\mathbf{b}^H, i\mathbf{b}^T)_m$  have very short wavelengths and small amplitudes compared with those of  $(\mathbf{b}^H, i\mathbf{b}^T)_0$ . The magnetic perturbations  $(\mathbf{h}, i\mathbf{t})_m$  themselves have very short wavelengths and very small amplitudes compared to those of  $(\mathbf{h}, i\mathbf{t})_0$ . We also find that  $(\mathbf{y}_1, \mathbf{y}_2)$  is hardly affected by the magnetic perturbations near the surface. It may be useful to note an approximate relation  $(\mathbf{h}, i\mathbf{t})_m \sim (\mathbf{b}^H, i\mathbf{b}^T)_m / \sqrt{\alpha}$ , which is derived from equation (34) assuming  $rd/dr \sim \sqrt{\alpha}$  for the Alfvénic perturbations. Note that in the region near the interface,  $(b_{l'=1}^H)_0 \sim \text{constant}$  and  $(ib_{l=2}^T)_0 \sim 0$  for the  $r$ -mode of  $m = 1$ , and  $(b_{l'=2}^H)_0 \sim 0$  and  $(ib_{l=3}^T)_0 \sim \text{constant}$  for the  $r$ -mode of  $m = 2$ , where  $(b_{l'}^H)_0$  and  $(ib_l^T)_0$  denote the non-Alfvénic parts of  $b_{l'}^H$  and  $ib_l^T$ , respectively. See §4 for a detailed discussion.

For the case of  $B_S = 10^{14}$  G, the real parts of the eigenfunctions of the  $r$ -mode of  $m = 2$  are plotted versus  $r/R$  in Figures 8 to 10, where we assume  $\bar{\Omega} = 0.1$  and  $k_{max} = 6$ , and we employ the amplitude normalization given by  $S_{l_1} = 1$  at the surface. The wavelengths and the amplitudes of the Alfvénic perturbations  $(\mathbf{b}^H, i\mathbf{b}^T)_m$  are much longer and much larger than those found for the case of  $B_S = 10^{12}$  G. It is interesting to note that the effect of the magnetic field on the eigenfunctions  $\mathbf{y}_1$  and  $i\mathbf{t}$  becomes apparent near the surface, as shown by the inlets in Figures 8 and 9. In Figure 11, to see the dependence of the Alfvénic perturbations on the value of  $k_{max}$ , we plot the real parts of  $(\mathbf{b}^H, i\mathbf{b}^T)$  for the  $m = 2$   $r$ -mode at  $\bar{\Omega} = 0.1$  for  $B_S = 10^{14}$  G, assuming  $k_{max} = 10$ . For this case, we have the eigenvalue  $(\kappa_R - \kappa_0)/\kappa_0 = 1.8 \times 10^{-5}$  and  $\kappa_I = 8.3 \times 10^{-7}$ , which is in good agreement with the value obtained for  $k_{max} = 6$ . Figure 11 shows that the wavelengths and the amplitudes of the Alfvénic perturbations  $(\mathbf{b}^H, i\mathbf{b}^T)_m$  for  $k_{max} = 10$  becomes shorter and smaller than those for the case of  $k_{max} = 6$ , which may reflect the property of the wavenumber  $k_r$  determined by  $ik_r \mathbf{Y}_m = A \mathbf{Y}_m$  that  $\max |\text{Re}(k_r)|$  increases as  $k_{max}$  increases.

#### 4 DISCUSSIONS AND CONCLUSIONS

Let us rewrite equation (2) as

$$-c_1 \bar{\omega}^2 \frac{\boldsymbol{\xi}}{r} = -\frac{r \nabla p'}{\rho g r} - \frac{\rho'}{\rho} - 2ic_1 \bar{\omega} \bar{\Omega} \times \frac{\boldsymbol{\xi}}{r} + \frac{2}{\beta V} \frac{(r \nabla \times \mathbf{B}') \times \mathbf{B}}{B_0^2}. \quad (44)$$

This equation may indicate that in the deep interior where the gas pressure dominates the magnetic pressure such that  $\beta \gg 1$ , the magnetic perturbations  $\mathbf{B}'$  have practically no influence on non-magnetic oscillations governed by equation (44), and they are determined solely by the induction equation (4). Using equation (4), we obtain

$$\nabla_H \cdot \mathbf{B}'_H = 2B_0 \left( r \frac{\partial}{\partial r} - 1 \right) \left[ -\cos \theta \nabla_H \cdot \frac{\boldsymbol{\xi}_H}{r} + \sin \theta \frac{\xi_\theta}{r} + \frac{1}{2} \left( \sin \theta \frac{\partial}{\partial \theta} + 2 \cos \theta \right) \frac{\xi_r}{r} \right], \quad (45)$$

$$(\nabla_H \times \mathbf{B}'_H)_r = 2B_0 \left[ \left( r \frac{\partial}{\partial r} - 1 \right) \left( -\cos \theta \left( \nabla_H \times \frac{\boldsymbol{\xi}_H}{r} \right)_r - \frac{im}{2} \frac{\xi_r}{r} \right) + \left( r \frac{\partial}{\partial r} - 1 - \frac{1}{2} \nabla_H^2 \right) \left( \sin \theta \frac{\xi_\phi}{r} \right) \right], \quad (46)$$

where

$$\mathbf{B}'_H = B'_\theta \mathbf{e}_\theta + B'_\phi \mathbf{e}_\phi, \quad \boldsymbol{\xi}_H = \xi_\theta \mathbf{e}_\theta + \xi_\phi \mathbf{e}_\phi, \quad \nabla_H = \mathbf{e}_\theta \frac{\partial}{\partial \theta} + \mathbf{e}_\phi \frac{1}{\sin \theta} \frac{\partial}{\partial \phi}. \quad (47)$$

Assuming

$$\xi_r = 0, \quad \xi_\theta = T_{l'} \frac{1}{\sin \theta} \frac{\partial}{\partial \phi} Y_{l'}^m, \quad \xi_\phi = -T_{l'} \frac{\partial}{\partial \theta} Y_{l'}^m, \quad (48)$$

for the  $r$ -mode of a given  $m$ , we obtain from equations (45) and (46)

$$b_{l'}^H = -\frac{2m}{l'(l'+1)} \left( r \frac{\partial}{\partial r} - 1 \right) \frac{iT_{l'}}{r}, \quad (49)$$

$$ib_l^T = -\frac{2l'}{l'+1} J_{l'+1}^m \left( r \frac{\partial}{\partial r} + \frac{l'-1}{2} \right) \frac{iT_{l'}}{r}, \quad (50)$$

where  $J_l^m = \sqrt{(l^2 - m^2)/(4l^2 - 1)}$  and  $l = l' + 1$  for odd modes. Since  $iT_{l'} \propto r$  for the  $r$ -mode of  $l' = m = 1$ , we have

$$(b_{l'}^H)_0 = \frac{iT_{l'}}{r} = \text{constant}, \quad (ib_l^T)_0 = 0, \quad (51)$$

and, since  $iT_{l'} \propto r^2$  for the  $r$ -mode of  $l' = m = 2$ , we have

$$(b_{l'}^H)_0 = 0, \quad (ib_l^T)_0 = -\frac{2}{\sqrt{7}} \frac{iT_{l'}}{r} \propto r. \quad (52)$$

Equations (51) and (52) for the non-Alfvénic parts of the magnetic perturbations are consistent with the eigenfunctions shown in Figures 4 and 7. Note that  $(b_{l'}^H)_0$  and  $(ib_l^T)_0$  are both non-zero for the  $r$ -modes of  $l' = m > 2$ .

Using a singular perturbation theory, we calculate low- $m$   $r$ -modes of a magnetized neutron star, assuming a magnetic dipole field whose axis is aligned with the axis of rotation. For an  $N = 1$  polytrope of mass  $M = 1.4M_\odot$  and radius  $R = 10^6$  cm, we find that the magnetic field of strength  $B_S \lesssim 10^{14}$  G has no significant influence on the modal properties of the  $r$ -modes with the frequency  $\bar{\omega} \sim \bar{\Omega}$  unless  $\bar{\Omega} \sim 0$ . We show that the magnetic perturbations  $\mathbf{B}'$  can be divided into Alfvénic and non-Alfvénic parts, where the non-Alfvénic part in the deep interior is governed by the induction equation (4). The Alfvénic part, on the other hand, has very short wavelengths in the interior. The radial wavenumber  $k_r$  of the Alfvénic perturbations is approximately given by  $k_r \sim t_A \omega$  where  $t_A$  denotes the traveling time of the Alfvén waves, and we have  $t_A \omega \gg 1$  beneath the stellar surface for the  $r$ -modes we consider in this paper. The Alfvénic perturbations become very short waves, being decoupled from the  $r$ -modes in the interior. This decoupling of the Alfvénic perturbations from the  $r$ -modes may cause a damping effect on the modes.

If we consider the growthtime  $\tau$  of the  $r$ -mode of  $m = 2$  driven unstable by current multipole gravitational radiation, we have

$$\tau \sim (3/4)^3 \tilde{\tau}_{l=2} \bar{\Omega}^{-6} \sim 1.4 \bar{\Omega}^{-6} \text{ sec}, \quad (53)$$

where we have used  $\tilde{\tau}_{l=2} = 3.31 \text{ sec}$ , and  $\bar{\Omega} = \Omega/\sigma_0$  with  $\sigma_0 = \sqrt{GM/R^3}$  (see, e.g, Yoshida & Lee 2000). Defining the growth timescale as  $\tau = -1/\omega_I$ , we have

$$\kappa_I \sim -5 \times 10^{-5} \bar{\Omega}^5, \quad (54)$$

where we have used  $\sigma_0 = 1.36 \times 10^4 \text{ s}^{-1}$  for  $M = 1.4M_\odot$  and  $R = 10^6$  cm. Thus, we have  $\kappa_I \sim -5 \times 10^{-10}$  for  $\bar{\Omega} = 0.1$  and  $\kappa_I \sim -1.2 \times 10^{-5}$  for  $\bar{\Omega} = 3/4$ . Comparing these values with the numbers  $\kappa_I$  given in Table 1, we may find that the  $r$ -mode instability can be damped by dissipative very short Alfvénic perturbations in the surface layer when the neutron stars with  $B_S \gg 10^{12}$  G are slowly rotating. For neutron stars in LMXB's, however, the strength of magnetic field is believed to be much weaker than  $10^{12}$  G, and the effects of the magnetic field on the  $r$ -mode instability will be unimportant.

In this paper, we have assumed that the axis of the magnetic field is aligned with the axis of rotation. If we lift this assumption, the problem will be much more complicated since the axisymmetry cannot be assumed and hence a perturbed quantity must be represented by a sum of terms proportional to  $Y_l^m$  over the indices  $l$  and  $m$ . The possible existence of a crustal layer in the envelope of a rotating magnetized neutron star also makes difficult the problem of the oscillations (e.g., McDermott, Van Horn, & Hansen 1988; Lee & Strohmayer 1996). Magnetic effects on the torsional oscillations of a neutron star with a solid crust have been discussed by Carroll et al (1986) and Messios, Papadopoulos, & Stergioulas (2001), but no effects of rotation have been included in these studies. If there exists a fluid ocean on the solid crust of a rotating neutron star, the magnetic effects on waves propagating in the ocean may be important observationally if the waves are responsible for burst oscillations found in neutron stars in LMXB systems (e.g., Lee 2004).

*Acknowledgments:* The author is very grateful to Prof. H. Saio for his illuminating discussion on the problem.

## REFERENCES

- Andersson N., 1998, ApJ, 502, 708  
 Andersson N., Kokkotas K.D., 2004, gr-qc/0403087  
 Bigot L., Provost J., Berthomieu G., Dziembowski W.A., Goode P.R., 2000, A&A, 356, 218  
 Bigot L., Dziembowski W.A., 2002, A&A, 391, 235  
 Biront D., Goossens M., Cousens A., Mestel L., 1982, MNRAS, 201, 619  
 Campbell C.G., Papaloizou J.C.B., 1986, MNRAS, 220, 577  
 Carroll B.W., Zweibel E.G., Hansen C.J., McDermott P.N., Savedoff M.P., Thomas J.H., Van Horn H.M., 1986, ApJ, 305, 767  
 Chandrasekhar S., 1970, Phys. Rev. Lett., 24, 611  
 Cunha M.S., Gough D., 2000, MNRAS, 319, 1020  
 Dziembowski W.A., Goode P. R., 1996, ApJ, 458, 338  
 Friedman J.L., Morsink S.M., 1998, ApJ, 502, 714  
 Friedman J.L., Schutz B.F., 1978a, ApJ, 221, 937  
 Friedman J.L., Schutz B.F., 1978b, ApJ, 222, 281  
 Ho W.C.G., Lai D., 2000, ApJ, 543, 386



- Kurtz D.W., 1990, ARA&A, 28, 607  
Lee U., 2004, ApJ, 600, 914  
Lee U., Saio H., 1986, MNRAS, 221, 365  
Lee U., Saio H., 1990, ApJ, 360, 590  
Lee U., Strohmayer T.E., 1996, A&A, 311, 155  
McDermott P.N., Van Horn H.M., Hansen C.J., 1988, ApJ, 325, 725  
Messios N., Papadopoulos D.B., Stergioulas N., 2001, MNRAS, 328, 1161  
Morsink S.M., Rezzani V., 2002, ApJ, 574, 908  
Owen B.J., Lindblom L., Cutler C., Schutz B.F., Vecchio A., Andersson N., 1998, Phys. Rev. D, 58, 084020  
Rezzolla L., Lamb F.K., Shapiro S.L., 2000, ApJ, 531 L139  
Roberts P.H., Soward A.M., 1983, MNRAS, 205, 1171  
Saio H., Gautschi A., 2004, MNRAS, 350, 485  
Schenk A.K., Arras P., Flanagan É. É., Teukolsky S.A., Wasserman I., 2001, Phys. Review D, 65, 024001  
Shibahashi H., Takata M., 1993, PASJ, 45, 617  
Takata M., Shibahashi H., 1995, PASJ, 47, 219  
Unno W., Osaki Y., Ando H., Saio H., Shibahashi H., 1989, Nonradial Oscillations of Stars. Univ. of Tokyo Press, Tokyo  
Yoshida S., Lee U., 2000a, ApJ, 529, 997  
Yoshida S., Lee U., 2000b, ApJS, 129, 353

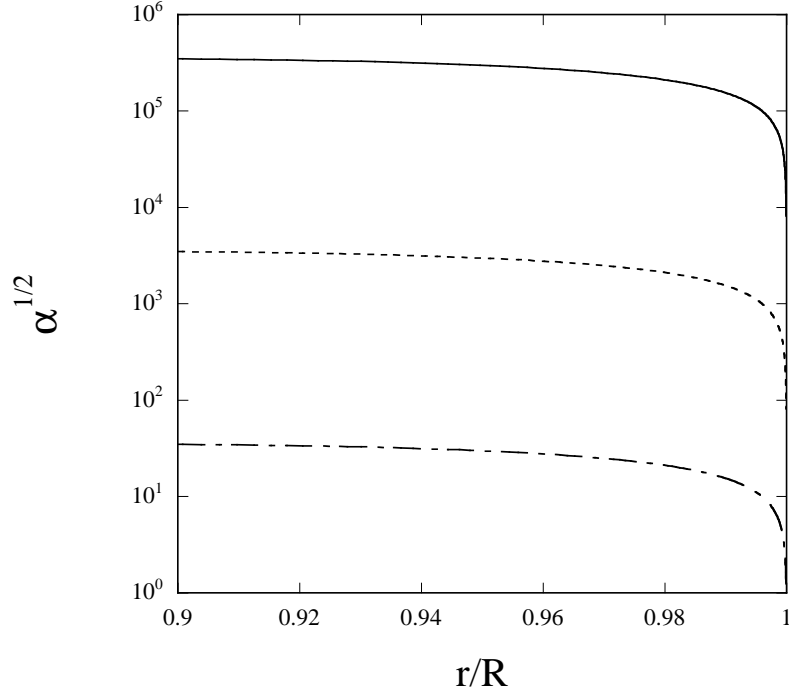


**Figure 1.** Plot of  $\alpha^{1/2}$  as a function of  $r/R$  for an  $N = 1$  polytrope of mass  $M = 1.4M_\odot$  and radius  $R = 10^6 \text{ cm}$ , where  $\bar{\omega} = \omega/\sqrt{GM/R^3} = 1$  is assumed. Solid, dashed, and dash-dotted lines are for the cases of  $B_S = 10^{12} \text{ G}$ ,  $10^{14} \text{ G}$ , and  $10^{16} \text{ G}$ , respectively.

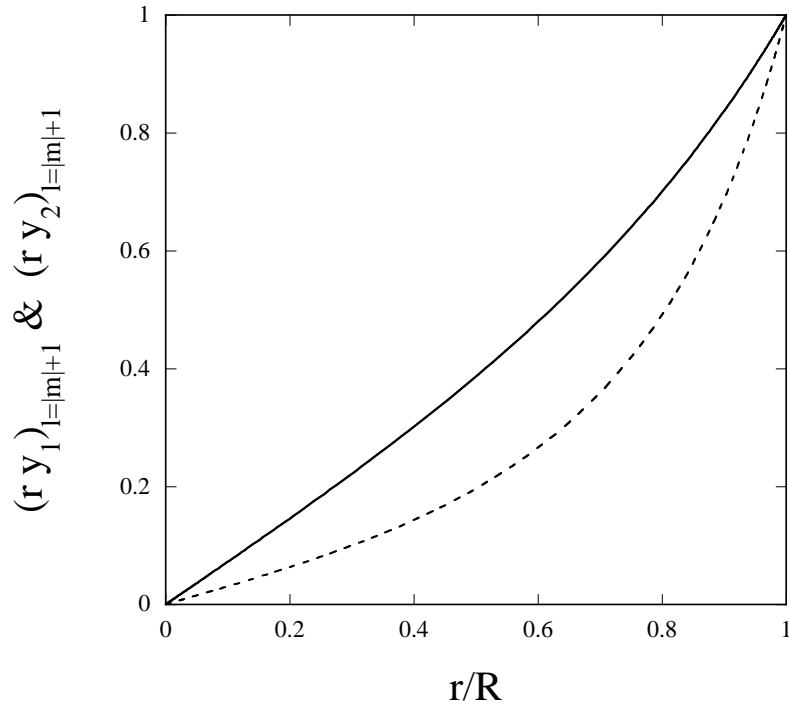


**Figure 2.** Eigenfunctions  $(ry_1)_{l=|m|+1}$  (solid curve) and  $(ry_2)_{l=|m|+1}$  (dashed curve) as a function of  $r/R$  for the  $r$ -mode of  $m = 1$  at  $\bar{\Omega} = 0.1$ , where  $B_S = 10^{12} \text{ G}$  and  $k_{max} = 6$ .

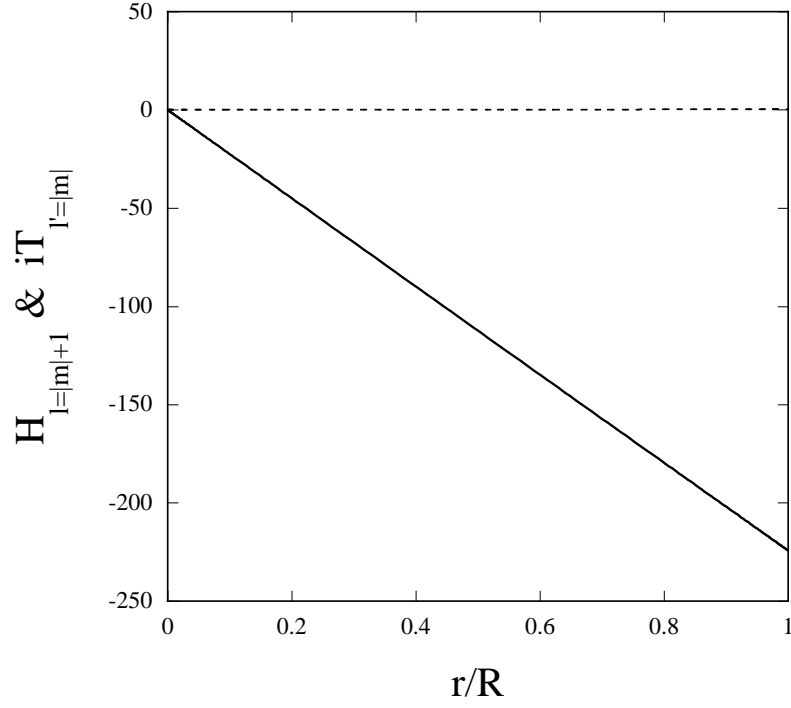


**Figure 3.** Eigenfunctions  $iT_{l'=|m|}$  (solid line) and  $H_{l=|m|+1}$  (dashed line) as a function of  $r/R$  for the  $r$ -mode of  $m = 1$  at  $\bar{\Omega} = 0.1$ , where  $B_S = 10^{12}\text{G}$  and  $k_{max} = 6$ .

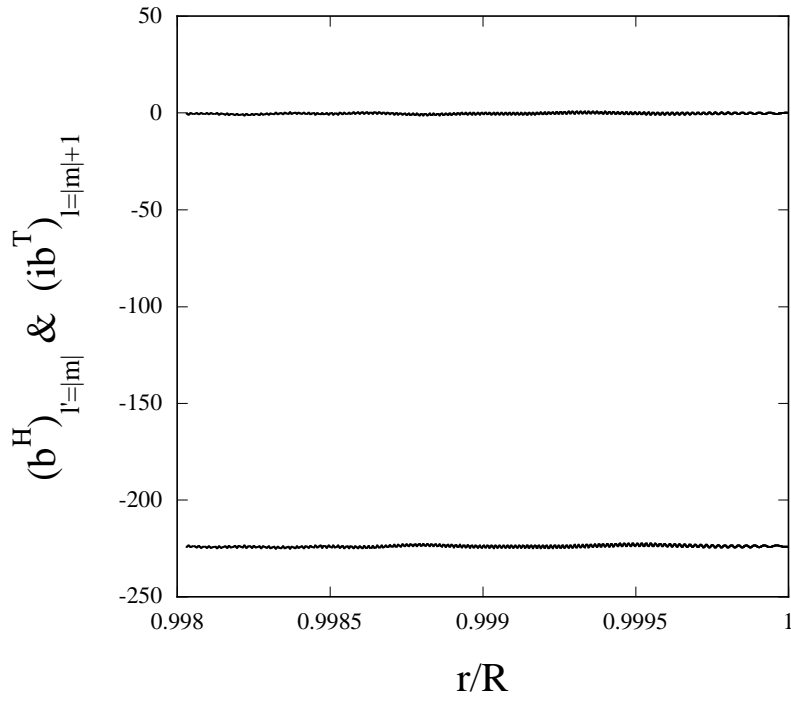


**Figure 4.** Eigenfunctions  $b_{l'=|m|}^H$  (lower curve) and  $ib_{l=|m|+1}^T$  (upper curve) as a function of  $r/R$  for the  $r$ -mode of  $m = 1$  at  $\bar{\Omega} = 0.1$ , where  $B_S = 10^{12}\text{G}$  and  $k_{max} = 6$ .

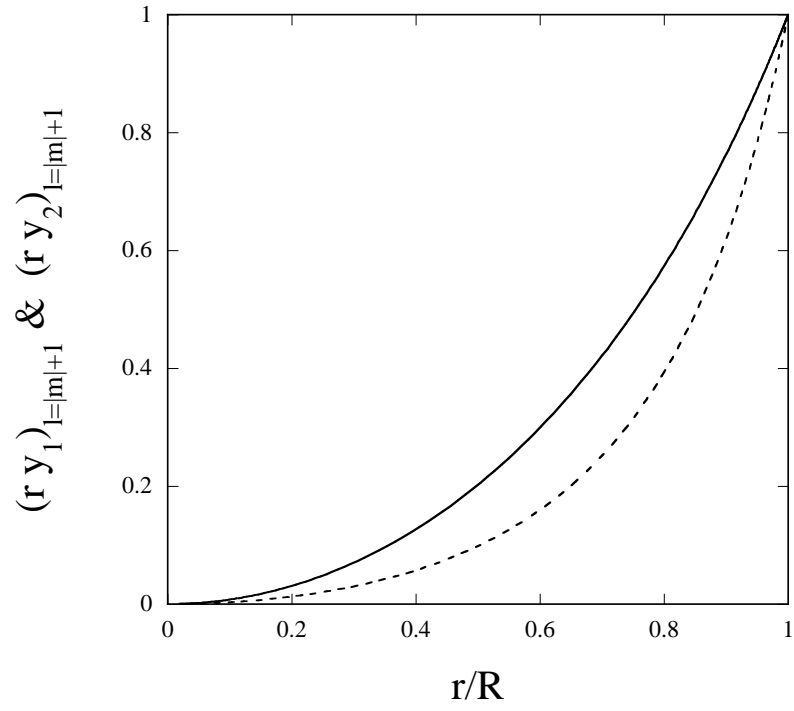


**Figure 5.** Same as Figure 2 but for  $m = 2$ .

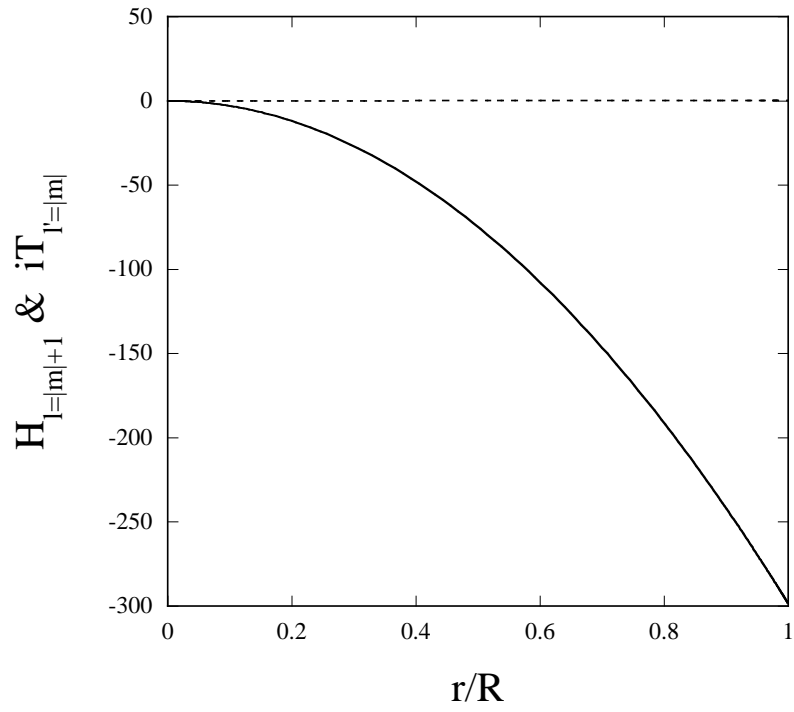


**Figure 6.** Same as Figure 3 but for  $m = 2$ .

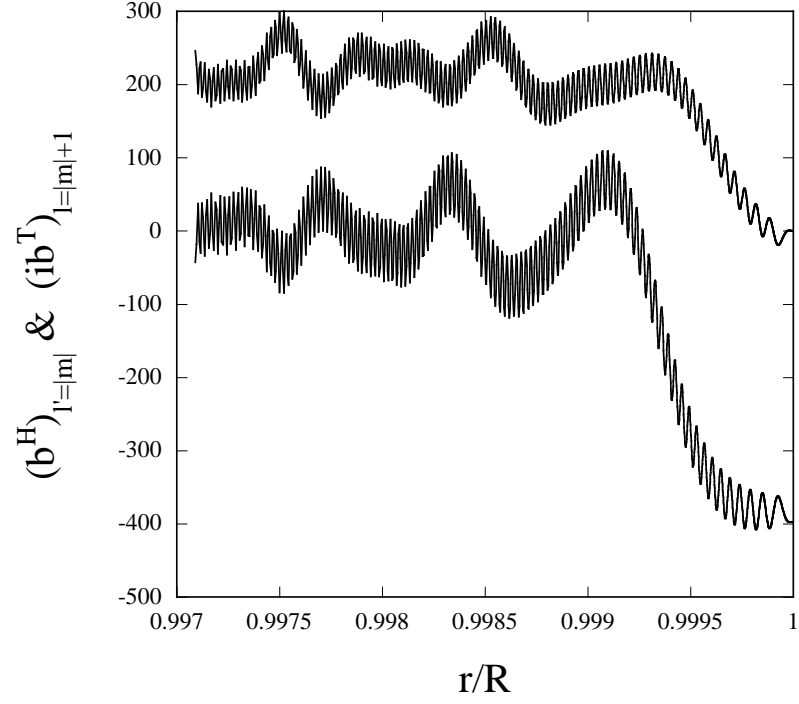


**Figure 7.** Same as Figure 4 but for  $m = 2$ .

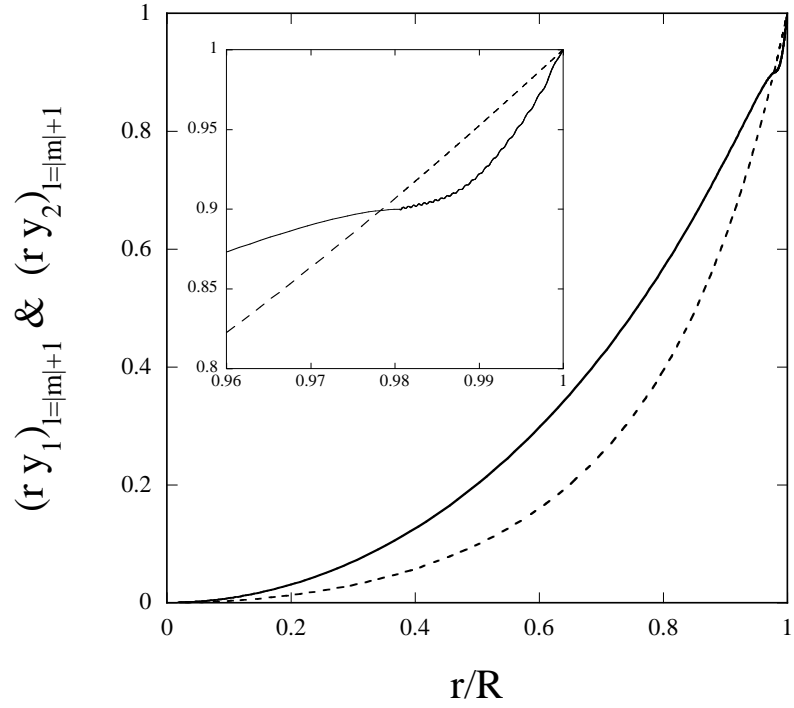


**Figure 8.** Same as Figure 5 but for  $B_S = 10^{14}$  G.

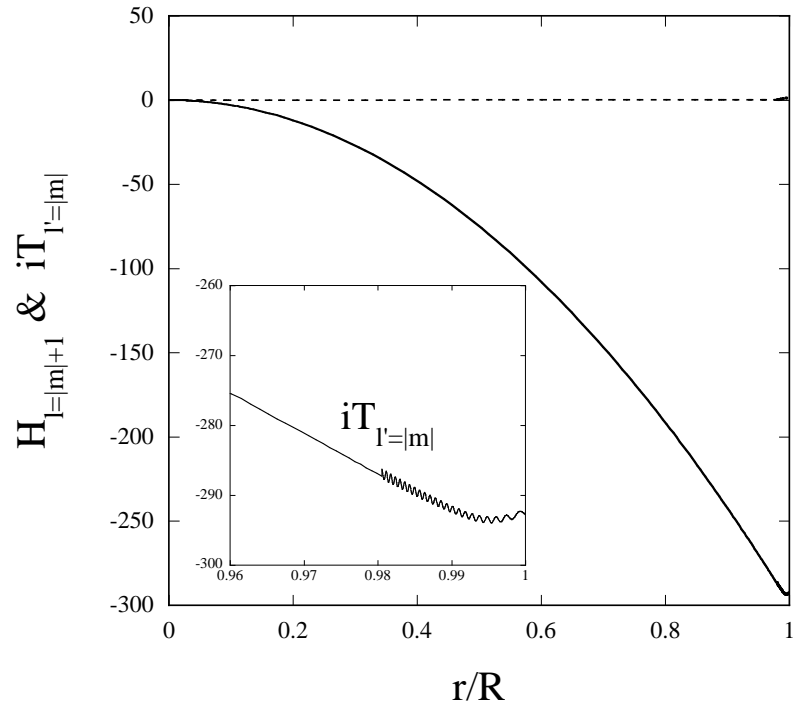


**Figure 9.** Same as Figure 6 but for  $B_S = 10^{14}$  G.

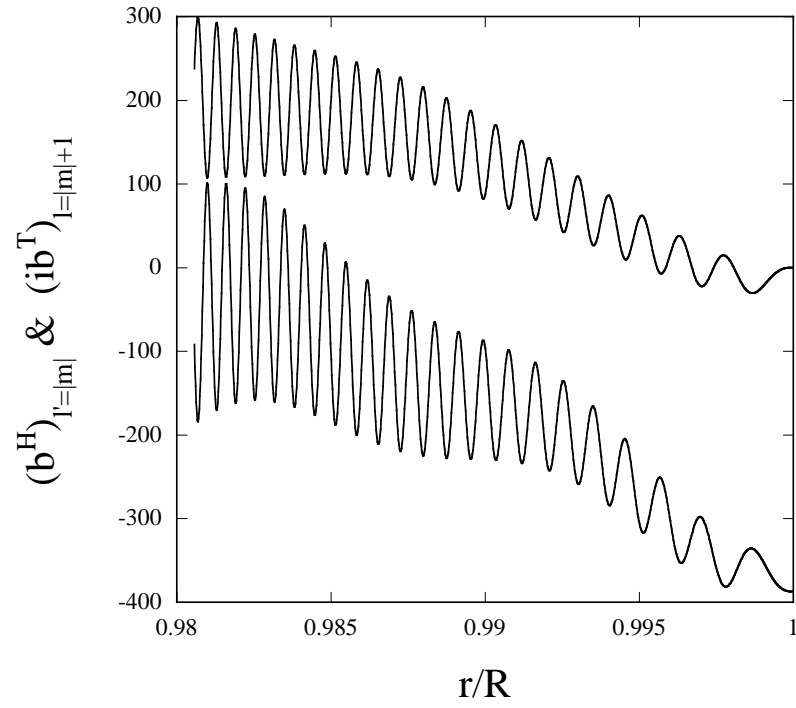


**Figure 10.** Same as Figure 7 but for  $B_S = 10^{14}$  G.

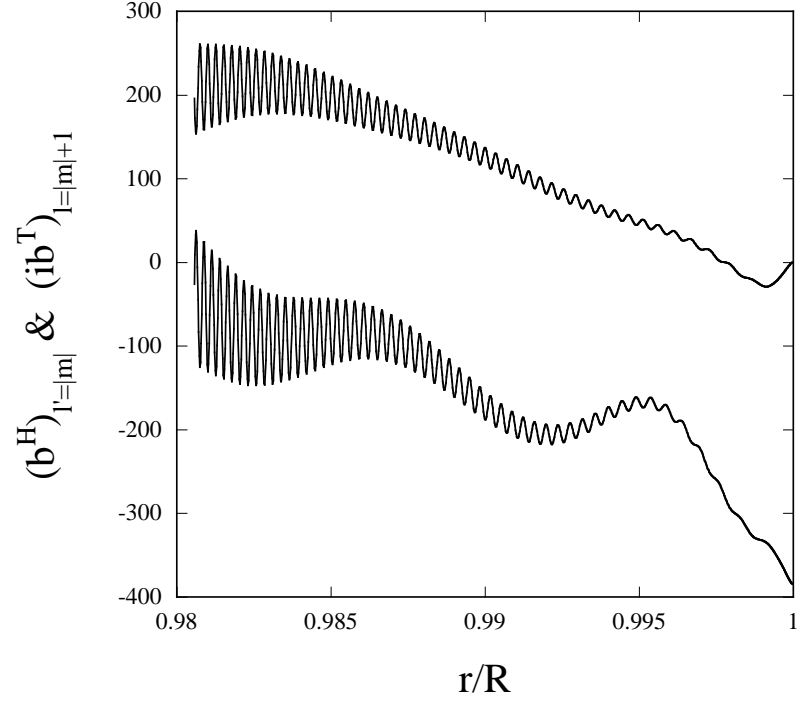


**Figure 11.** Same as Figure 10 but for  $k_{max} = 10$ .